pared in the cosmid cloning vector pJSR1, which was constructed by ligating a 1.6-kb Bgl II fragment containing the bacteriophage lambda *cos* site from pHC79 [B. Hohn and J. Collins, *Gene* **11**, 291 (1980)] into the Bgl II site of pRR54 [R. C. Roberts, R. Burioni, D. R. Helinski, *J. Bacteriol.* **172**, 6204 (1990)].

23. A 1.7-kb Bam HI fragment isolated from plasmid pMS150 containing the *toxA* gene (*24*) and a 3.0-kb Bam HI–Pst I fragment from plasmid pSL2 containing the *plcS* gene [S. Lory and P. C. Tai, *Gene* **22**, 95 (1983)] were used to probe the UCBPP-PA14 genomic library in pJSR1 (*22*).
24. S. Lory, M. S. Strom, K. Johnson, *J. Bacteriol.* **170**, 714 (1988).
25. The oligonucleotides 5′-GCTAGTAGTCGATGACC-3′ and 5′-GTGGCATCAACCATGC-3′ were designed on the basis of the sequence of the *gacA* gene (*19*) and were used to amplify a 625-base pair (bp) product containing the *gacA* gene of *P. fluorescens*, which in turn was used to probe the UCBPP-PA14 genomic library in pJSR1 (*22*).
26. A 3.6-kb Bgl II–Bam HI fragment containing the *plcS* gene was subcloned into the Bam HI site of pBR322 and then mutagenized by insertion of a gentamicin-resistance gene cassette into the Xho I site of the *plcS* gene to construct pLGR201. The gentamicin-resistance gene cassette is a 1.8-kb Bam HI fragment from plasmid pH1JI [R. A. Rubin, *Plasmid* **18**, 84 (1987)] provided by S. Lory. The Xho I site is located approximately in the middle of the *plcS*-coding region (*17*). A 1.6-kb Bam HI fragment containing the *toxA* gene was subcloned into pBR322 and then mutagenized by introduction of the gentamicin cassette into the Bgl II site of the *toxA* gene to construct plasmid pLGR202. The Bgl II site is located near the middle of the *toxA*-coding region (*24*). A 2.4-kb Hind III–Eco RI fragment containing the *gacA* gene was subcloned into pBR322 and then mutagenized by insertion of the gentamicin cassette into the Bam HI site of *gacA* to construct the plasmid pLGR203. Approximately 300 bp of the presumptive *gacA* gene was sequenced (from the Bam HI site) and was found to exhibit 89% identity at the nucleotide level to the *P. fluorescens gacA* gene (*19*). The Bam HI site is located near the middle of the *P. aeruginosa gacA* gene-coding region.
27. Plasmids pLGR201, pLGR202, and pLGR203 were used for gene replacement of *plcS*, *toxA*, and *gacA* genes, respectively, as described [L. G. Rahme, M. N. Mindrinos, N. J. Panopoulos, *J. Bacteriol.* **170**, 575 (1991)], by first selecting for resistance to gentamicin (30 μg/ml) and then screening for sensitivity to carbenicillin (300 μg/ml). Three independent *gacA* mutants were constructed. The structures of all of the resulting marker exchange mutations were verified by DNA blot analysis. The UCBPP-PA14 *plcS* mutant exhibited reduced hemolytic activity on blood agar plates (*17*) and the UCBPP-PA14 *gacA* mutant exhibited sensitivity to ultraviolet (UV) radiation (*21*) and did not produce extracellular cyanide (*19*). None of these three mutations had any detectable effect on either the growth rate or the final density of the bacteria in vitro compared to the wild type in either rich or minimal media.
28. Statistical significance for mortality data was determined by the χ^2 test with Yates'correction. Differences between groups were considered statistically significant at $P \leq 0.05$. All the mutants were significantly different from the wild type (*plcS* and *toxA*, $P \leq 0.05$; *gacA*, $P \leq 0.00005$).
29. A 6.1-kb Bam HI fragment containing the *plcSR* operon of strain UCBPP-PA14 was subcloned into the Bam HI site of plasmid pRR54 and used for genetic complementation studies. A 2.4-kb Eco RI–Eco RV fragment containing only the *toxA* gene from *P. aeruginosa* strain PAK was cloned in the Sma I site of pRR54 and used for complementation studies. An 8.7-kb DNA fragment containing the *gacA-uvrC* operon of strain UCBPP-PA14 was cloned in the polylinker of pRR54 and used for complementation studies. In addition, a 2.4-kb Hind III–Eco RI fragment containing the UCBPP-PA14 *gacA* gene was cloned into pBR322 and used to replace the *gacA* gene interrupted by the gentamicin cassette with a wild-type copy of *gacA*. In the mouse model, the lethality elicited by the complemented *plcS* and *toxA* mutants and the reconstructed *gacA*$^+$ strain was not statistically different from that of the UCBPP-PA14 wild type. The complemented *gacA* mutant was UV-resistant, synthesized cyanide, and elicited approximately 50% lethality in the mouse model as compared to 0% for the *gacA* mutant. In the plant model, the complemented *plcS* and *toxA* mutants and the reconstructed *gacA*$^+$ strain elicited disease symptoms similar to those of wild-type UCBPP-PA14, the reconstructed *gacA*$^+$ strain grew to wild-type levels, the final population level of the complemented *gacA* mutant was approximately 1.5 orders of magnitude less than that of the wild type, and the complemented *toxA* and *plcS* mutants grew to a level that was approximately 0.5 order of magnitude less than that of the wild type. The partial complementation observed in some of these experiments may be due to gene dosage effects.
30. The *toxA* gene is not known to be part of an operon. Because the *plcS* gene is situated in an operon with *plcR*, a gene that regulates *plcS* expression, and the *gacA* gene is situated in an operon with *uvrC*, the reduced pathogenicity phenotypes of the *plcS* and *gacA* mutants may be due to polar effects on the downstream *plcR* or *uvrC* genes.
31. We thank N. Panopoulos for helpful suggestions at the initial stage of this work; M. Schroth, S. Kominos, S. Lory, and J. Goldberg for the *P. aeruginosa* strains and plasmids; and S. Calderwood for helpful advice. Supported by a grant from Shriners Hospitals for Crippled Children and by a grant from Hoechst AG to Massachusetts General Hospital.

23 December 1994; accepted 24 May 1995

Reversal of Raf-1 Activation by Purified and Membrane-Associated Protein Phosphatases

Paul Dent, Tomas Jelinek, Deborah K. Morrison, Michael J. Weber, Thomas W. Sturgill*

The Raf-1 protein kinase participates in transduction of mitogenic signals, but its mechanisms of activation are incompletely understood. Treatment of human Raf-1 purified from insect Sf9 cells co-expressing c-H-Ras and Src(Y527F) (in which phenylalanine replaces tyrosine at residue 527) with either serine-threonine or tyrosine phosphatases resulted in enzymatic inactivation of Raf-1. Inactivation of purified Raf-1 was blocked by addition of either the 14-3-3ζ protein or heat shock protein 90. Loading of plasma membranes from transformed cells with guanosine triphosphate (GTP) resulted in inactivation of endogenous or exogenous Raf-1; inactivation was blocked by inclusion of protein phosphatase inhibitors. These results suggest the existence of protein phosphatases in the cell membrane that are regulated by GTP and are responsible for Raf-1 inactivation.

The proto-oncogene product Raf-1 is a serine-threonine protein kinase that functions in one or more protein kinase cascades important for mitogenic signaling (*1*). Raf-1 phosphorylates and activates mitogen-activated protein (MAP) kinase kinase (MKK, also known as MEK), the specific activator of MAP kinase. MAP kinase in turn phosphorylates several regulatory proteins (*2*) in the cytoplasm and nucleus to alter the program of transcription and translation required for mitogenesis.

The mechanism of Raf-1 activation is unclear. Activation of Raf-1 in vivo occurs at the plasma membrane and is dependent on association with the guanosine triphosphate (GTP)–bound form of Ras (*1*). Artificial targeting of Raf-1 to the plasma membrane in vivo bypasses Ras dependence and results in an enhancement of Raf-1 enzymatic activity (*3*). Raf-1 is also activated in vitro by purified plasma membranes from transformed cells in an adenosine triphosphate (ATP)–dependent manner (*4*). However, the association of purified Raf-1 and Ras proteins in the presence of ATP in vitro is not sufficient for Raf-1 activation, suggesting that an ATP-dependent mechanism such as phosphorylation exists for Raf-1 activation at the plasma membrane.

Raf-1 is phosphorylated in quiescent cells, and its phosphorylation increases at several sites in cells stimulated with mitogens (*5–7*). Threonine-268, serines-43, -259, -499, and -621 (*5*), and tyrosines-340 and -341 have been identified as phosphorylation sites in Raf-1 (*6*). Mitogenic stimulation of fibroblasts with platelet-derived growth factor or phorbol esters increases phosphorylation of Ser^{259} (*5*) and Ser^{499} (*6*), respectively. Mutation of Ser^{259} or Ser^{499} to Ala does not inhibit the activation of Raf-1 in insect Sf9 cells by Ras and Src(Y527F) (*5*); the effects of these mutations on activation by phorbol esters are unclear (*7*). Mutation of Ser^{621}, which is phosphorylated in quiescent fibroblasts and in Sf9 cells expressing Raf-1 alone, results in a protein that cannot be activated (*5*). Furthermore, mutation of Tyr^{340} and Tyr^{341}, the major sites of tyrosine phosphorylation, to Phe also results in a Raf-1 pro-

P. Dent and T. W. Sturgill, Howard Hughes Medical Institute and Markey Center for Cell Signaling, Departments of Medicine and Pharmacology, University of Virginia, Charlottesville, VA 22908, USA.
T. Jelinek and M. J. Weber, Department of Microbiology, University of Virginia, Charlottesville, VA 22908, USA.
D. K. Morrison, Advanced Bioscience Laboratories Inc. Basic Research Program, National Cancer Institute–Frederick Cancer Research and Development Center, Frederick, MD 21702, USA.
*To whom correspondence should be addressed.

tein that is not activated in Sf9 cells by Ras and Src(Y527F) (6).

Although these data are consistent with activation by phosphorylation, they do not prove that any of the Raf-1 phosphorylation events observed are regulatory rather than ancillary. The Raf-1 electrophoretic mobility shift induced by phosphorylation does not always correlate temporally with its enzymatic activation (8, 9). Indeed, efforts to inactivate Raf-1 from Sf9 cells by incubation with mixtures of various protein phosphatases have been inconclusive (4, 10).

To investigate the possible regulation of Raf-1 by phosphorylation, we purified recombinant Raf-1 from Sf9 cells so that it was substantially free of associated proteins (11, 12). The purities of preparations obtained by three different procedures were compared by SDS–polyacrylamide gel electrophoresis (PAGE) and silver staining (Fig. 1). Wild-type Raf-1 or catalytically inactive Raf-1(K375M) (in which Lys^{375} is replaced by Met) proteins purified by nickel-chelate chromatography through a COOH-terminal $(His)_6$-tag were impure. In contrast, NH_2-terminally FLAG-tagged Raf-1 purified by immunoaffinity chromatography (FLAG–Raf-1) and untagged Raf-1 purified by specific adsorption to Ras-GTP (SAR–Raf-1) were nearly homogeneous. The Raf-1–associated heat shock protein 90 (Hsp90) (8, 13) and p50 (8, 13) and 14-3-3 proteins (14, 15) were effectively removed from FLAG–Raf-1 and SAR–Raf-1 preparations by these procedures (Fig. 1).

Preparations of affinity-purified FLAG–Raf-1 and SAR–Raf-1 that were activated as a result of co-expression in Sf9 cells with c-H-Ras and Src(Y527F) were treated with protein–serine-threonine phosphatases 1 (PP1) and 2A (PP2A), protein-tyrosine phosphatase 1B (PTP1B), or all three phosphatases (16) (Fig. 2). Raf-1 activity was assessed directly by phosphorylation of MKK1 or indirectly in a coupled reaction by phosphorylation of catalytically inactive $p42^{mapk}$(Lys^{52} → Arg, or K52R). SAR–Raf-1 was inactivated by treatment with either the serine-threonine or tyrosine phosphatases (Fig. 2A). Inactivation was not apparent when specific phosphatase inhibitors were included during phosphatase treatment. Catalytically inactive PTP1B(Cys^{216} → Ser, or C216S) also failed to inactivate SAR–Raf-1 (17). The decrease in MKK phosphorylating activity was accompanied by a similar decrease in phosphorylation of $p42^{mapk}$(K52R) in the coupled assay, indicating that the MKK phosphorylation catalyzed by the Raf-1 preparation was regulatory. Similar experiments were performed with FLAG–Raf-1 and different preparations of the same phosphatases. FLAG–Raf-1 was almost completely inactivated by either the serine-threonine or tyrosine phosphatases (Fig. 2B). PTP1B treatment also resulted in a decrease in immunoreactivity of FLAG–Raf-1 with antibodies to phosphotyrosine (17). Differences in the extent of Raf-1 inactivation were apparent between experiments and are likely attributable to variability in the extent of removal of the associated 14-3-3 and Hsp90 proteins, as well as to the use of different phosphatase preparations. These results demonstrate an apparent requirement for both serine-threonine and tyrosine phosphorylation for Raf-1 activity, and they are consistent with a previous study showing that treatment of immunoprecipitated Raf-1 with PTP1B decreased autokinase activity (6). Inactivation by PTP1B demonstrates that tyrosine phosphorylation is causally related to Raf-1 activation. Because phosphorylation of Ser^{621} may be required constitutively, inactivation of Raf-1 by serine-threonine phosphatases may be attributable to dephosphorylation of Ser^{621}, in addition to

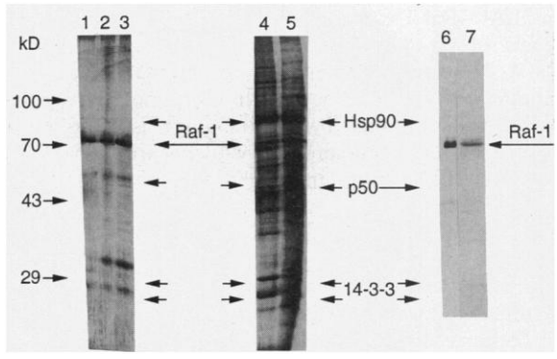

Fig. 1. Silver-stained SDS-polyacrylamide gel of purified preparations of FLAG–Raf-1, $(His)_6$–Raf-1, and SAR–Raf-1 from Sf9 cells. Raf-1 proteins were expressed from recombinant baculoviruses in Sf9 cells either alone (inactive) or with (active) recombinant baculoviruses encoding c-H-Ras and Src(Y527F) (11). Proteins [1 μg or 10 μg for $(His)_6$-tagged Raf-1 proteins] from each preparation were subjected to SDS-PAGE (11% gels) and silver staining. Lanes: 1, inactive FLAG–Raf-1; 2, active FLAG–Raf-1; 3, FLAG–Raf-1(K375M); 4, inactive $(His)_6$–Raf-1; 5, $(His)_6$–Raf-1(K375M); 6, inactive SAR–Raf-1; 7, active SAR–Raf-1. $(His)_6$–, FLAG–, and SAR–Raf-1 were purified by single-step affinity chromatography on Ni^{2+}-agarose, anti-FLAG immunoglobulin G–agarose, or glutathione-S-transferase–Ras-GTP, respectively (12). Molecular size standards (in kilodaltons), Raf-1, and the Raf-1–associated Hsp90, p50, and 14-3-3 proteins are indicated by arrows.

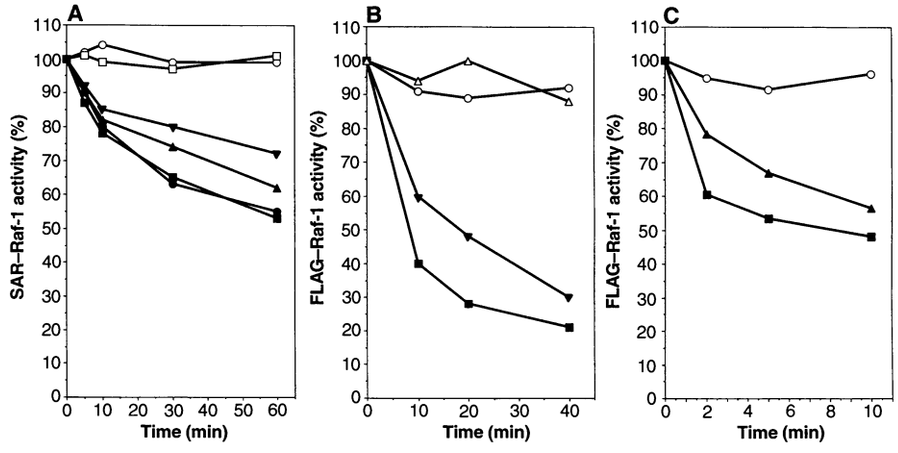

Fig. 2. Inactivation of SAR–Raf-1 or FLAG–Raf-1 catalyzed by either protein-serine-threonine or protein-tyrosine phosphatases. Preparations of active Raf-1 proteins (5 μg of total protein) were treated with active (solid symbols) or inactivated (open symbols) protein phosphatases at 30°C for various times (16). At the indicated times, portions of the reaction mixture were removed and assayed for Raf-1 activity (16). (**A**) Inactivation of SAR–Raf-1 by treatment with PP1 and PP2A (▼); PTP1B (▲); or PP1, PP2A, and PTP1B (●, ■) demonstrated, by assays of MKK1 phosphorylation (■) or MKK1 activation (▼, ▲, ●). Controls: inactivated PTP1B (○, □); controls for inactivated PP1 and inactivated PP2A are similar, but not plotted. Incorporation of ^{32}P into $(His)_6$-MKK1 or $p42^{mapk}$(K52R) substrate was quantified by Cerenkov radiation. Data are means (n = 3) from a representative experiment. Incorporation at 0 min (100%) was 8600 and 67,900 cpm for MKK1 and $p42^{mapk}$(K52R) phosphorylation, respectively. (**B**) Inactivation of MKK1 phosphotransferase activity of FLAG–Raf-1 by treatment with PP1 and PP2A (▼) or with PTP1B (■). Controls: inactivated PP1, PP2A, and PTP1B (△), and untreated FLAG–Raf-1 (○). Data are means (n = 4) from a representative experiment. MKK1 phosphorylation at 0 min (100%) was 42,600 ± 2500 cpm (mean ± SD). (**C**) Comparison of the efficacies of the PP1 catalytic subunit (■) and the PP2A heterodimer (A:C) (▲) in inactivation of FLAG–Raf-1. Control: inactivated PP1 and PP2A (○). Data are means (n = 3) from a representative experiment. MKK1 phosphorylation at 0 min was 39,600 ± 2100 cpm (mean ± SD).

or independent of dephosphorylation of other regulatory serine or threonine residues.

FLAG–Raf-1 activated by co-expression with Ras alone was inactivated by treatment with PTP1B but not by treatment with PTP1B inactivated by vanadate (*17*). The ability of PTP1B to inactivate FLAG–Raf-1 expressed with Ras in the absence of Src suggests that a portion of FLAG–Raf-1 from cells co-expressing Ras is tyrosine phosphorylated. Protein immunoblot analysis with antibodies to phosphotyrosine confirmed the presence of phosphotyrosine in FLAG–Raf-1 expressed with Ras, but at levels substantially lower than for FLAG–Raf-1 expressed with Src (*17*). A Raf-1 mutant containing Phe at the tyrosine phosphorylation sites Tyr^{340} and Tyr^{341} is not activated by co-expression with Ras in Sf9 cells (*6*). Our results suggest that tyrosine phosphorylation may be required for Raf-1 activation in the absence of Src.

With equal amounts of glycogen phosphorylase phosphatase activity, the PP1 catalytic subunit was twice as efficacious as the PP2A heterodimer in inducing inactivation of FLAG–Raf-1 (Fig. 2C). The specific activity of PP1 with phosphorylase as substrate is at least five times greater than that of PP2A (*18*). Thus, the relative phosphatase activities of PP1 and PP2A toward Raf-1 may differ by as much as an order of magnitude.

PP1 inactivates a syntide 2 peptide kinase activity present in Raf-1 immunoprecipitates from insulin-treated cells (*19*), but syntide 2 is not a substrate for Raf-1 (*20, 21*). Similarly, a study of Raf-1 inactivation by the tyrosine phosphatase CD45 (*22*) used a peptide that is also not a substrate for Raf-1 (*21*). The potential for Raf-1 to be deactivated by protein phosphatases has been previously studied, but the results were inconclusive because of the substrates used.

Preparations of $(His)_6$-tagged Raf-1 were not inactivated by treatment with either serine-threonine or tyrosine phosphatases. The factor or factors responsible for the difference in susceptibility of these Raf-1 preparations are not known, but one major difference between the preparations is the complexity of proteins copurifying with Raf-1 (Fig. 1). Proteins in the 14-3-3 family bind to both active and inactive Raf-1 (*17, 21*) and have been suggested to participate in Raf-1 activation (*14, 15*).

The effects of the Raf-1–associated proteins 14-3-3ζ and Hsp90 on the susceptibility of FLAG–Raf-1 to inactivation by protein phosphatases were examined (Fig. 3). Addition of either recombinant 14-3-3ζ or purified human brain Hsp90 before phosphatase treatment blocked Raf-1 inactivation by a mixture of PP1 and PP2A or by PTP1B. The inhibition of inactivation appeared not to result from inhibition of the protein phosphatases themselves, because neither 14-3-3ζ nor Hsp90 affected phosphatase activities toward other ^{32}P-labeled substrates (*17*). Inhibition of Raf-1 inactivation by 14-3-3ζ or Hsp90 is thus likely to result from their association with Raf-1. The 14-3-3 proteins inhibit the dephosphorylation of phosphohistone by PC12 cell extracts (*23*), and 14-3-3ζ_2 binds directly to the phosphorylated form, but not to the dephosphorylated form, of tryptophan hydroxylase (*24*).

Addition of 14-3-3ζ to FLAG–Raf-1 isolated from Sf9 cells infected with only the Raf-1 virus did not result in Raf-1 enzymatic activation (*17*). In contrast, addition of 14-3-3ζ to active FLAG–Raf-1 resulted in a 39 ± 8% (mean ± SD, $n = 4$) increase in FLAG–Raf-1 activity. The ability of 14-3-3ζ both to augment the activity of active

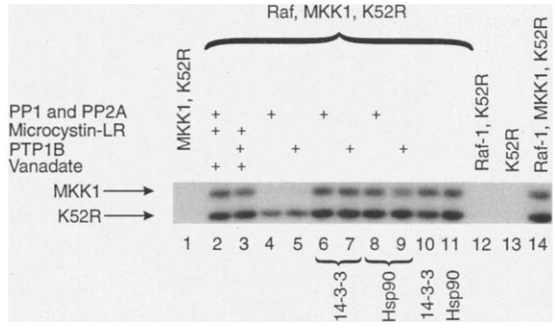

Fig. 3. Effects of 14-3-3ζ and Hsp90 on inactivation of FLAG–Raf-1 by protein phosphatases. Active FLAG–Raf-1 (1 μg) was incubated (15 min, 4°C) with or without 5 μg of recombinant 14-3-3ζ or 5 μg of purified human brain Hsp90 (StressGen, Victoria, British Columbia, Canada) in a total volume of 25 μl. Active FLAG–Raf-1 was then treated with protein phosphatases as described (*16*) for 60 min and assayed (15 min, 30°C) for the ability both to phosphorylate and to activate MKK1. MKK1 and $p42^{mapk}$(K52R) phosphorylation by active FLAG–Raf-1 (lane 14) were 126,000 and 198,400 cpm, respectively; control incorporation with inactivated phosphatases (lane 2) was equivalent. MKK1 and $p42^{mapk}$(K52R) autophosphorylation (lanes 1 and 13) were 710 and 470 cpm, respectively.

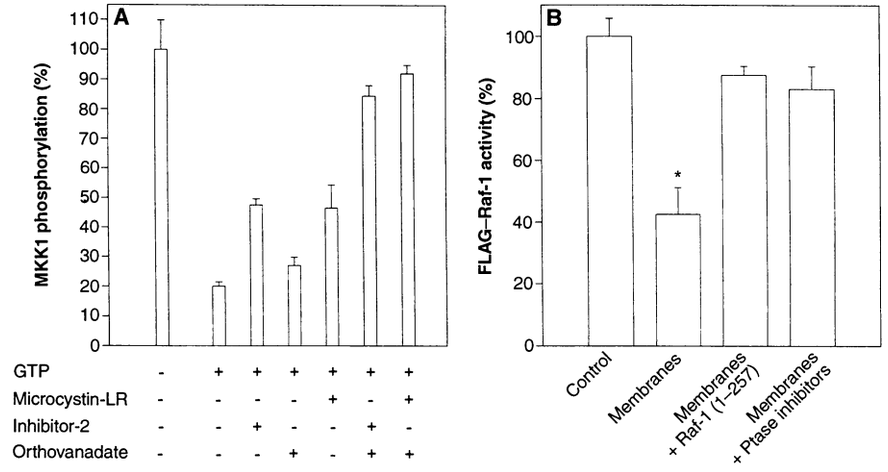

Fig. 4. GTP-stimulated inactivation of endogenous and exogenous Raf-1 by membrane-associated protein phosphatases in plasma membrane preparations from transformed cells. (**A**) Effects of protein phosphatase inhibitors on the GTP-induced decrease in endogenous membrane-associated MKK-phosphorylating activity. Plasma membranes were incubated (30°C, 15 min) in the absence or presence of 1 mM GTP and protein phosphatase inhibitors as indicated and then isolated by centrifugation (*25*). Portions (5 μl containing 5 μg of total protein) were assayed (30°C, 15 min) for MKK-phosphorylating activity (*16*). Incorporation of ^{32}P into MKK1 (750 ± 150 cpm, $n = 3$) catalyzed by endogenous Raf-1 in the absence of GTP and phosphatase inhibitors was defined as 100%. (**B**) Inactivation of exogenous active FLAG–Raf-1 by association with GTP-loaded plasma membranes from transformed cells. Plasma membranes from transformed cells were incubated with GTP in the absence or presence of phosphatase (Ptase) inhibitors and isolated by centrifugation (*25*). Portions (5 μl, 5 μg of total protein) of resuspended membranes were treated (15 min on ice), or mock-treated, with 1 μg of a bacterially expressed NH_2-terminal fragment of Raf-1 [Raf-1(1–257)] to block interaction of active FLAG–Raf-1 with v-Ras in the membranes (*4*). Active FLAG–Raf-1 (1 μg of total protein) was incubated for 5 min at 30°C in a total volume of 12 μl with membranes, and portions (10 μl) of the reaction mixture were assayed for MKK-1–phosphorylating activity in the presence of protein phosphatase inhibitors (*16*). Data are expressed as a percentage of ^{32}P incorporation catalyzed by FLAG–Raf-1 in the absence of membranes [47,600 ± 3100 cpm ($n = 4$)] (control); MKK1 autophosphorylation (750 ± 150 cpm) and ^{32}P incorporation into membranes (6700 ± 1000) were negligible by comparison. Data are means ± SD for three to four monolayers for (A) and (B); the asterisk (*) indicates $P < 0.05$ for comparison to control values.

Raf-1 and to block its inactivation may explain some of the stimulatory effects of 14-3-3 overexpression on Raf-1 activity in vivo. However, a defined role for 14-3-3 in Raf-1 activation under physiological conditions has not been demonstrated.

We tested whether mechanisms for Raf-1 inactivation were present in plasma membranes. Preparations of plasma membranes from transformed fibroblasts contain activated Raf-1 (*4*). Incubation of such membranes with GTP resulted in a reduction in the activity of membrane-associated Raf-1 (*25*) (Fig. 4A) without loss of Raf-1 from the membranes, as assessed by protein immunoblot analysis (*17*). Inactivation of endogenous Raf-1 was blocked by the addition of protein phosphatase inhibitors (Fig. 4A). Microcystin-LR is a potent inhibitor of PP1 and PP2A, whereas inhibitor-2 specifically inhibits PP1 but not PP2A. Addition of inhibitors of both PP1 and tyrosine phosphatases (inhibitor-2 and sodium vanadate, respectively) was necessary to prevent the decrease in endogenous Raf-1 activity (Fig. 4A). Addition of 5 μg of recombinant 14-3-3ζ alone also prevented the decrease in endogenous Raf-1 activity (*17*). Incubation of plasma membranes from untransformed cells with GTP resulted in a similar decrease in the much smaller amount of endogenous MKK activator activity (<10% of that in transformed cells) present in these membranes (*17*). We also incubated exogenous active FLAG–Raf-1 with GTP-treated or untreated membranes from transformed cells (Fig. 4B). Incubation with GTP-treated membranes resulted in a 55% inactivation of active FLAG–Raf-1, which was blocked by protein phosphatase inhibitors. Guanosine 5′-O-(3-thiotriphosphate) or 5′-guanylyl-imidodiphosphate (GMPPNP), but not guanosine diphosphate, substituted for GTP in inducing inactivation of both endogenous and exogenous Raf-1 (*17*). Although the membrane preparations are enriched for plasma membranes, we cannot exclude the participation of a membrane phosphatase from another cell compartment.

Inactivation of exogenous Raf-1 was also blocked by prior incubation of membranes with a recombinant NH_2-terminal fragment of Raf-1 (Fig. 4B). Plasma membrane localization of active Raf-1 thus appears to be important for GTP-stimulated inactivation in vitro. However, the ability of GTP to stimulate inactivation of endogenous Raf-1 suggests that the effect requires more than colocalization to the membrane and may be mediated by activation of a protein phosphatase. Both tyrosine phosphatases (such as CD45 and PTP1B) and forms of the serine-threonine phosphatase PP1 are localized to the plasma membrane and may participate in Raf-1 inactivation. A protein-tyrosine phosphatase activity present in plasma membranes is regulated by a pertussis toxin–sensitive, GTP-dependent mechanism (*26*). PP1, but not PP2A, is associated with particulate fractions, including plasma membranes, presumably by an unidentified membrane-targeting subunit (*27*). Colocalization of a protein phosphatase with its substrates is a key factor regulating its ability to catalyze dephosphorylation both in vitro and in vivo (*27*). Membrane localization of active Raf-1 enhances its inactivation and is thus consistent with this concept.

We conclude that phosphorylation of Raf-1 is causal to activation because dephosphorylation results in its enzymatic inactivation. PP1 and PTP1B are highly specific for phosphoserine-phosphothreonine and phosphotyrosine, respectively. In particular, the structure of the catalytic pocket of PTP1B, as determined by crystallography, is too deep to permit dephosphorylation of phosphoserine or phosphothreonine residues (*28*). Thus, phosphorylation of Raf-1 at both tyrosine and serine-threonine sites is required for enzymatic activity stimulated by Ras and Src(Y527F), whereas dephosphorylation of either type of site is sufficient to cause inactivation. Our results further suggest that serine-threonine phosphorylation of Raf-1 in the absence of tyrosine phosphorylation is insufficient for Raf-1 kinase activity.

REFERENCES AND NOTES

1. J. Avruch, X. F. Zhang, J. M. Kyriakis, *Trends Biochem. Sci.* **19**, 279 (1994); N. G. Williams and T. M. Roberts, *Cancer Metast. Rev.* **13**, 105 (1994).
2. R. J. Davis, *J. Biol. Chem.* **268**, 14553 (1993); T. A. J. Haystead *et al.*, *ibid.* **269**, 23185 (1994).
3. S. J. Leevers, H. F. Paterson, C. J. Marshall, *Nature* **369**, 411 (1994); D. Stokoe, S. G. Macdonald, K. Cadwallader, M. Symons, J. F. Hancock, *Science* **264**, 1463 (1994).
4. P. Dent and T. W. Sturgill, *Proc. Natl. Acad. Sci. U.S.A.* **91**, 9544 (1994).
5. D. K. Morrison *et al.*, *J. Biol. Chem.* **268**, 17309 (1993).
6. J. R. Fabian, I. O. Daar, D. K. Morrison, *Mol. Cell. Biol.* **13**, 7170 (1993).
7. W. Kolch *et al.*, *Nature* **364**, 249 (1993); C. E. Whitehurst *et al.*, *J. Biol. Chem.* **270**, 5594 (1995).
8. M. Wartmann and R. J. Davis, *J. Biol. Chem.* **269**, 6695 (1994).
9. M. L. Samuels, M. J. Weber, J. M. Bishop, M. McMahon, *Mol. Cell. Biol.* **13**, 6241 (1993).
10. S. Traverse *et al.*, *Oncogene* **8**, 3175 (1993); S. Traverse and P. Cohen, *FEBS Lett.* **350**, 13 (1994).
11. P. Dent *et al.*, *Biochem. J.* **303**, 105 (1994).
12. Wild-type and kinase-defective (K375M) $(His)_6$-tagged human Raf-1 proteins were expressed and purified by Ni^{2+}-chelate chromatography as described (*11*). To express FLAG-tagged human Raf-1, we infected Sf9 cells with FLAG–Raf-1 recombinant virus [estimated multiplicity of infection (MOI), 10] either alone or together with recombinant viruses for c-H-Ras and Src(Y527F) (each at an MOI of 2). (The FLAG epitope tag is a product of IBI-Kodak, New Haven, CT.) Forty-eight hours after infection, cells were homogenized in 40 ml of buffer A [450 mM tris-Cl (pH 7.9 at 4°C), 0.5% NP-40, 0.1% sodium deoxycholate, 0.05% SDS, 0.5 mM EDTA, 0.5 mM EGTA, 1 mM sodium orthovanadate, 5 mM sodium pyrophosphate, 25 mM sodium β-glycerophosphate, 5 mM benzamidine, 1 mM phenylmethylsulfonyl fluoride (PMSF), egg white trypsin inhibitor (0.1 mg/ml), 10% (v/v) glycerol, and 0.1% 2-mercaptoethanol]. The homogenate was centrifuged (5000*g*, 4°C, 10 min) and the resulting supernatant was adsorbed to 0.5 ml of anti–FLAG M2 immunoglobulin G–agarose (IBI-Kodak) at 4°C for 2 hours. The agarose beads were washed twice with 50 ml of buffer A and twice with 50 ml of buffer B [25 mM tris-Cl (pH 7.9 at 4°C), 0.1 mM EDTA, 0.1 mM EGTA, 0.01% NP-40, 1 mM benzamidine, 0.1 mM PMSF, 10% (v/v) glycerol, and 0.1% 2-mercaptoethanol], and FLAG–Raf-1 was eluted by gentle agitation overnight at 4°C with 5 ml of buffer B containing FLAG peptide (0.1 mg/ml). The beads were again washed with 5 ml of buffer B, which was pooled with the initial eluate. Eluted FLAG–Raf-1 was dialyzed against buffer B containing 50% (v/v) glycerol, omitting NP-40, and was stored at −20°C. SAR–Raf-1 was purified by a procedure to be described in detail elsewhere (T. Jelinek, P. Dent, T. Sturgill, M. Weber, in preparation) that includes specific adsorption to the GTP-bound form of a glutathione-S-transferase–Ras fusion protein, washing, and elution based on the Mg^{2+}-stimulatable guanosine triphosphatase activity of c-H-Ras in buffer B containing 10 mM $MgCl_2$. The $(His)_6$–Raf-1 preparations were estimated to be only 5% pure, whereas Raf-1 usually constituted ≥60% of total protein in the FLAG–Raf-1 or SAR–Raf-1 preparations. FLAG-tagged and SAR–Raf-1 preparations, in contrast to $(His)_6$-tagged Raf-1 preparations, were not stable to freezing and thawing.
13. L. F. Stancato *et al.*, *J. Biol. Chem.* **268**, 21711 (1993).
14. H. Fu *et al.*, *Science* **266**, 126 (1994).
15. E. Freed, M. Symons, S. G. Macdonald, F. McCormick, R. Ruggieri, *ibid.* **265**, 1713 (1994); K. Irie *et al.*, *ibid.*, p. 1716; W. J. Fantl *et al.*, *Nature* **371**, 612 (1994); K. Shimizu *et al.*, *J. Biol. Chem.* **269**, 22917 (1994); S. Li *et al.*, *EMBO J.* **14**, 685 (1995).
16. Active FLAG–Raf-1 or SAR–Raf-1 was incubated at 30°C (total volume, 50 μl) in buffer C [25 mM tris-Cl (pH 7.5 at 30°C), 0.1 mM EDTA, 0.1 mM EGTA, 1 mM benzamidine, 0.01% NP-40, 10% (v/v) glycerol, 1 mM dithiothreitol] containing homogeneous preparations of PP1 catalytic subunit [1.5 mU/ml, or 3.0 mU/ml (Fig. 2C)] [D. L. Brautigan and C. L. Shriner, *Arch. Biochem. Biophys.* **275**, 44 (1989)], PP2A catalytic subunit or A:C heterodimer [1.5 mU/ml, or 3.0 mU/ml (Fig. 2C)] [H. Usui *et al.*, *J. Biol. Chem.* **258**, 10455 (1983)], PTP1B (5000 U/ml, 0.1 mg/ml) [D. Barford, J. C. Keller, A. J. Flint, N. K. Tonks, *J. Mol. Biol.* **239**, 726 (1994)], or PTP1B(C216S) (0.1 mg/ml). Control reactions contained equal amounts of phosphatases inactivated by prior incubation for 15 min at 30°C in a solution containing 10 μM microcystin-LR (Calbiochem, La Jolla, CA), 0.2 mM sodium vanadate, and 25 mM sodium β-glycerophosphate (pH 7.4 at 30°C). Reactions were initiated by addition of active or inactivated phosphatases. At various times, equal portions (10 μl) were removed from the reaction mixture and added to 90 μl of buffer D [25 mM sodium β-glycerophosphate (pH 7.4 at 30°C), 10 μM microcystin-LR, 0.2 mM sodium orthovanadate, 0.5 mM $MnCl_2$, 15 mM $MgCl_2$, 0.2 mM [γ-^{32}P]ATP (5000 cpm/pmol)] for measurement of phosphotransferase activity. After incubation for 1 min at 30°C, phosphorylation reactions were initiated by addition of 3 μl (3 μg) of $(His)_6$-MKK1 in buffer B. In some experiments, after 11 min, 20 μl (20 μg) of $p42^{mapk}$(K52R) in buffer B was added. Reactions were terminated after 16 min by addition of 10 μl of 5× SDS-PAGE sample buffer. Proteins were resolved by SDS-PAGE, stained with Coomassie blue, and subjected to autoradiography. Stained protein bands of $(His)_6$-MKK1 and $p42^{mapk}$(K52R) were excised and ^{32}P incorporation determined by measurement of Cerenkov radiation.
17. P. Dent, T. Jelinek, M. J. Weber, T. Sturgill, unpublished data.
18. L. M. Ballou and E. H. Fischer, *Enzymes*, P. D. Boyer and E. G. Krebs, Eds. (Academic Press, Orlando, FL, 1986), vol. 27, p. 311.
19. K. S. Kovacina, *J. Biol. Chem.* **265**, 12115 (1990).
20. T. Force *et al.*, *Proc. Natl. Acad. Sci. U.S.A.* **91**, 1270 (1994).

21. D. K. Morrison, unpublished data.
22. B. C. Turner, N. K. Tonks, U. R. Rapp, J. C. Reed, *Proc. Natl. Acad. Sci. U.S.A.* **90**, 5544 (1993).
23. F. Chen and P. D. Wagner, *FEBS Lett.* **347**, 128 (1994).
24. Y. Furukawa *et al.*, *Biochem. Biophys. Res. Commun.* **194**, 144 (1993).
25. Plasma membranes were purified as described by flotation on discontinuous sucrose gradients (*4*), resuspended (1 mg/ml) in buffer E [25 mM Hepes (pH 7.4 at 30°C), 10 mM EDTA, 10 mM EGTA] containing the specified mix of protease inhibitors (*4*), kept on ice, and used immediately. Equal portions of resuspended plasma membranes from v-*ras*–transformed NIH 3T3 cells and v-*src*–transformed Raf-1 cells (5 to 10 100-mm dishes, each) were combined and sonicated (three 20-s bursts) on ice in a bath sonicator (model G112SP1G; Laboratory Supply, Hicksville, NY). Sonicated plasma membranes (0.1 ml, 0.1 mg of total protein) were then incubated (30°C, 15 min) in the absence or presence of 1 mM GTP and protein phosphatase inhibitors (final concentrations: 10 μM microcystin-LR, 100 μM inhibitor-2, 0.2 mM sodium orthovanadate). Membranes from each condition were centrifuged (100,000*g*, 15 min, 4°C) in an Airfuge (Beckman, Palo Alto, CA) and resuspended in buffer E to a volume of 0.1 ml. No appreciable losses of total membrane or Raf-1 protein occurred. Raf-1 is not appreciably dissociated from immobilized Ras-GTP by chelators (*17*), consistent with the observation that dissociation of guanine nucleotide from Ras is negligible in the absence of competing nucleotide [A. Hall and A. J. Self, *J. Biol. Chem.* **261**, 10963 (1986)].
26. M. G. Pan, T. Florio, P. Stork, *Science* **256**, 1215 (1992).
27. M. J. Hubbard and P. Cohen, *Trends Biochem. Sci.* **18**, 172 (1993).
28. D. Barford, A. J. Flint, N. K. Tonks, *Science* **263**, 1397 (1994).
29. We thank P. Cohen and D. Brautigan for PP1; T. Haystead and D. Brautigan for PP2A; N. Tonks for PTP1B and catalytically inactive PTP1B; D. Pallas for recombinant 14-3-3ζ; K. Zeller, L. A. Vincent, and C. Harrison for technical assistance; and D. Brautigan for helpful discussions. Supported by the Howard Hughes Medical Institute and by grants from NIH to T.W.S. (DK41077) and to M.J.W. (GM47322), and from the American Cancer Society to T.W.S. (BE69D) and by contract to D.K.M. (N01-CO-46000). P.D. is a postdoctoral fellow of the Juvenile Diabetes Foundation International.

23 January 1995; accepted 26 April

Requirement for TNF-α and IL-1α in Fetal Thymocyte Commitment and Differentiation

Juan Carlos Zúñiga-Pflücker,* Di Jiang, Michael J. Lenardo

CD25 expression occurs early in thymocyte differentiation. The mechanism of induction of CD25 before T cell receptor rearrangement and the importance of this mechanism for T cell development are unknown. In a thymus reconstitution assay, tumor necrosis factor α (TNF-α) and interleukin-1α (IL-1α), two cytokines produced within the thymic microenvironment, induced CD25 expression on early immature thymocytes. Either TNF-α or IL-1α was necessary for further thymocyte maturation and $CD4^+CD8^+$ differentiation. In irradiated mice reconstituted with $CD117^+CD25^+$ thymocytes, commitment to the T cell lineage was marked by the loss of precursor multipotency.

An important question in developmental biology is the nature of the molecular signals that occur between interacting tissues during organogenesis. In the immune system, the thymus is formed when the rudimentary thymic stroma is colonized by fetal liver–derived hematopoietic stem cells at day 12 of fetal life, and it provides the necessary elements for the commitment and differentiation of stem cells into T cells (*1*, *2*). During early fetal thymic development, it is unclear when commitment to the T lineage occurs. Newly arrived thymic lymphocyte precursors express CD117 (c-kit), which is the receptor for stem cell factor (SCF) and identifies cells from the fetal liver, bone marrow, and thymus that display hematopoietic stem cell function (*3*). The loss of CD117, beginning approximately at day 15, correlates with initiation of T cell receptor (TCR) β-chain rearrangement (*3*). The next step in thymocyte maturation is associated, in both mouse and human, with the expression of CD25 (IL-2 receptor α chain) (*4*); however, it is apparent that binding of IL-2 is not required for normal thymus development (*5*). Nevertheless, $CD25^+$ thymocytes predominate at days 14 and 15 of mouse fetal development (Fig. 1A) and express gene regulatory proteins and surface proteins that are characteristic of antigen-activated mature T cells (*6*). Although mature T cells express CD25 after TCR ligation (*7*), CD25 expression by $CD117^+$ immature thymocytes occurs before TCR rearrangement. We therefore investigated the molecular mechanism of CD25 induction and its significance in thymocyte differentiation and commitment to the T lineage.

To study CD25 induction, we prepared

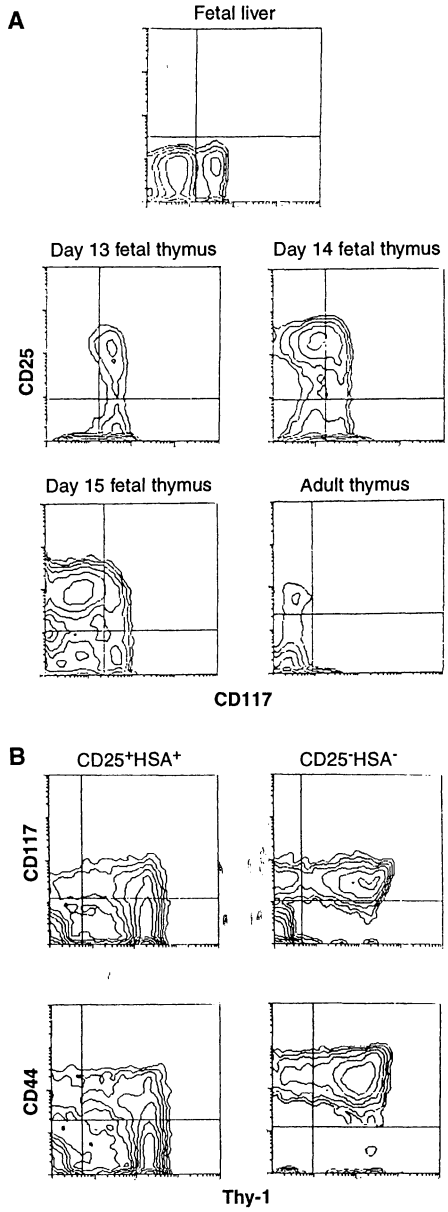

Fig. 1. T cells go through a $CD117^+CD25^+$ stage during early fetal thymic development. (**A**) CD25 and CD117 expression as a function of time in mouse fetal thymic development and in day 13 fetal liver (*15*). Percent staining for CD117 versus CD25 is given for the upper left (UL), upper right (UR), lower left (LL), and lower right (LR) areas of the flow cytometry plots. Fetal liver cells, UL, 0.0%; UR, 0.5%; LL, 78.7%; and LR, 20.7%. Day 13 fetal thymus, UL, 4.7%; UR, 27.0%; LL, 21.8%; and LR, 46.5%. Day 14 fetal thymus, UL, 35.1%; UR, 24.2%; LL, 22.6%; and LR, 18.1%. Day 15 fetal thymus, UL, 59.1%; UR, 9.4%; LL, 24.3%; and LR, 7.2%. Adult thymus, UL, 11.6%; UR, 1.8%; LL, 81.2%; and LR, 5.45%. (**B**) Phenotype of the HSA^-CD25^- SCID immature thymocytes prepared by treatment with antibody and complement elimination of later thymocyte stages (*16*). Percent staining for Thy-1 versus CD117: $CD25^+HSA^+$ thymocytes (not treated), UL, 1.9%; UR, 18.2%; LL, 14.3%; and LR, 65.5%. $CD25^-HSA^-$ thymocytes (treated), UL, 7.8%; UR, 45.6%; LL, 44.2%; and LR, 2.3%. Percent staining for Thy-1 versus CD44: $CD25^+HSA^+$ thymocytes, UL, 2.3%; UR, 18.7%; LL, 6.7%; and LR, 72.3%. $CD25^-HSA^-$ thymocytes, UL, 13.7%; UR, 83.4%; LL, 1.2%; and LR, 1.7%.

Laboratory of Immunology, National Institute of Allergy and Infectious Diseases, Bethesda, MD 20892, USA.

*Present address: University of Toronto, Department of Immunology, Medical Sciences Building, Toronto, Ontario M5S 1A8, Canada.